Structural and Magnetic Properties of Epitaxial $Fe_{25}Pt_{75}$

G. Mankey – University of Alabama

et al.

Citation of published version:

Lu, Z., Walock, M., LeClair, P., Mankey, G. (2009): Structural and Magnetic Properties of Epitaxial $Fe_{25}Pt_{75}$. *Journal of Vacuum Science and Technology A*, 27(4).
DOI: https://doi.org/10.1116/1.3143668

Structural and magnetic properties of epitaxial $Fe_{25}Pt_{75}$

Z. Lu, M. J. Walock, P. R. LeClair, G. J. Mankey, P. Mani, D. Lott, F. Klose, H. Ambaye, V. Lauter, M. Wolff, A. Schreyer, H. M. Christen, and B. C. Sales

Citation: Journal of Vacuum Science & Technology A **27**, 770 (2009); doi: 10.1116/1.3143668
View online: https://doi.org/10.1116/1.3143668
View Table of Contents: https://avs.scitation.org/toc/jva/27/4
Published by the American Vacuum Society

Structural and magnetic properties of epitaxial $Fe_{25}Pt_{75}$

Z. Lu, M. J. Walock, P. R. LeClair, and G. J. Mankey[a)]
MINT Center, University of Alabama, Tuscallosa, Alabama 35487

P. Mani
Western Digital, Fremont, CA 94536

D. Lott
GKSS Research Center, Max-Planck Strasse 1, 21502 Geesthacht, Germany

F. Klose
Australian Nuclear Science and Technology Organisation, Menai, New South Wales 2234, Australia

H. Ambaye and V. Lauter
Spallation Neutron Source, Oak Ridge National Laboratory, Oak Ridge, Tennessee 37831

M. Wolff
Department of Physics, Ruhr-University Bochum, 44780 Bochum, Germany

A. Schreyer
GKSS Research Center, Max-Planck Strasse 1, 21502 Geesthacht, Germany

H. M. Christen and B. C. Sales
Oak Ridge National Laboratory, Oak Ridge, Tennessee 37831

(Received 3 October 2008; accepted 4 May 2009; published 29 June 2009)

Epitaxial films of $Fe_{25}Pt_{75}$ have a number of different magnetic phases as a function of temperature and chemical order. For example, chemically ordered epitaxial films have two distinct antiferromagnetic phases at temperatures below ~160 K and exhibit paramagnetism above that temperature. In sharp contrast, chemically disordered epitaxial films are ferromagnetic with a Curie temperature that is greater than 400 K. It is demonstrated that by varying the substrate temperature during growth, epitaxial films with varying degrees of chemical order can be produced and it is possible to produce an alloy with the same composition throughout the film with a modified magnetic structure. The authors used polarized neutron reflectivity to gauge the magnetism of a $Fe_{25}Pt_{75}$ sample produced with a periodic variation in the growth temperature and showed that the sample exhibits a reduced Curie temperature of approximately 300 K as compared to bulk $Fe_{25}Pt_{75}$. © *2009 American Vacuum Society.* [DOI: 10.1116/1.3143668]

I. INTRODUCTION

The goal of this work is to learn to control magnetic ordering on the nanoscale. This can be accomplished by studying thin film layers of $FePt_3$, a material that has a remarkable property that, depending on the degree of chemical order, a ferromagnetic (FM) and an antiferromagnetic (AF) state can coexist at the same temperature. Direct magnetic exchange coupling at the interface between an antiferromagnet and a ferromagnet can result in a shift of the magnetic hysteresis curve along the field axis. This exchange bias effect (for recent reviews, see Refs. 1–3) is essentially a magnetic pinning effect leading to a unidirectional anisotropy. If an FM/AF interface sample is cooled in an external magnetic field from a temperature below the Curie temperature T_C of the FM through the Néel temperature T_N of the AF ($T_C > T_{start} > T_N \Rightarrow T_C > T_N > T_{end}$), the interfacial AF spins may align in a preferential orientation relative to the FM spins as the AF order sets in. If subsequently, after completion of the cooling process, the direction of the external field is reversed, the AF/FM interface spins exert a torque upon reversing FM interface spins which effectively stabilizes their field-cooled direction. Macroscopically, the exchange bias effect leads to an offset of the center of the hysteresis loop by an amount called the exchange bias field.

In recent years, significant research efforts were aimed at exploring the exchange bias effect in thin film structures because of its implementation in devices such as spin valves in magnetoresistive sensors and nonvolatile magnetic random access memory cells (for recent reviews, see Refs. 4 and 5). While the basic mechanisms leading to exchange bias are qualitatively well understood, a quantitative understanding of the effect is challenging in view of the frequently used complex chemical structures and electronic interactions at the actual FM/AF thin film interfaces. In order to test the applicability of theoretical models, it would be highly desirable to investigate the AF/FM interfaces that are structurally as perfect as possible. In this regard, $FePt_3$ is a remarkable exception because, depending on the degree of chemical order, it can, at the same temperature and composition, develop either FM or AF order.[6,7]

The crystal structure of $FePt_3$ is similar to Cu_3Au, which is a prototype for a chemical order-disorder transition. Stoi-

a)Electronic mail: gmankey@mint.ua.edu

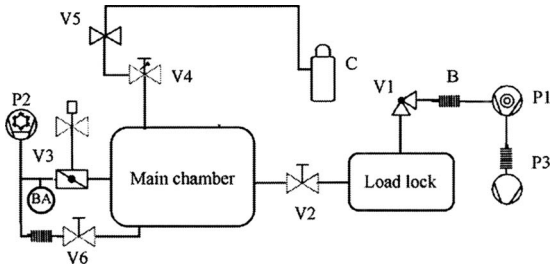

FIG. 1. Vacuum plant of the ADAM sputtering chamber.

chiometric $FePt_3$ in perfectly chemically ordered face-centered-cubic (fcc) L12 structure shows an antiferromagnetic order below T_N=170 K. In this structure, the chemical order corresponds to the Fe atoms occupying the corners and Pt atoms located at the faces of the cubic cell. The Fe moments ($m_{Fe}=3.3\mu_B$ extrapolated to $T=0$ K) order on (110) alternating ferromagnetic subsheets, while the Pt atoms carry a small moment ($m_{Pt}<0.2\mu_B$).

The AF ordered magnetic phase of $FePt_3$ is very sensitive to plastic deformation, resulting in a chemical disorder.[6,7] Plastic deformation with consequential increased dislocation densities can be obtained by cold working the chemically ordered alloy, which, in turn, leads to Fe atoms occupying face-centered positions rather than corner positions in the fcc ordered lattice.[8] As a result, the positive exchange between next neighbor Fe atoms introduces a tendency to FM order. Completely disordered $FePt_3$, has a fcc structure in which each lattice site is occupied by, on average, $\frac{1}{4}$ Fe and $\frac{3}{4}$ Pt atoms, where the atomic fractions represent probabilities. Chemically disordered bulk $FePt_3$ orders FM at temperatures below about 425 K.

In this article, we demonstrate that the chemical ordering of epitaxial films can be controlled by varying the substrate temperature during growth. The design of this experiment was stimulated by a prior result where we studied a superlattice of $CoPt_3/FePt_3$. It was expected that such a superlattice would constitute a FM/AF system since the perfectly ordered films are FM for $CoPt_3$ and AF for $FePt_3$. However, a detailed analysis of the data showed that a portion of the $FePt_3$ contributed to the ferromagnetism of the sample.[9] These results show the tantalizing result that a properly designed sample may exhibit a new result, namely, a material that is exchange biased with itself. Our preliminary results are promising and show that a film produced by modulating the substrate temperature during growth has a significant ferromagnetic fraction with a Curie temperature near 300 K.

II. EXPERIMENT

The sputter deposition of the films was carried out in the Alabama Deposition of Advanced Materials (ADAM) sputtering chamber which is shown schematically in Fig. 1. The deposition was performed in the main chamber, which was evacuated using a CTI cryogenics Cryotorr 10 cryopump. A load lock chamber allowed samples to be transferred from and to the main chamber quickly. The load lock was pumped using a 160 l/s Balzers turbopump, backed by a GE rotary vane pump. Initial pumping of the main chamber was through the load lock to a crossover pressure of about 1×10^{-4} mbar. The base pressure of the main vacuum chamber after an overnight bake was less than 1×10^{-8} mbar as measured with a Kurt J. Lesker model IG200 ionization gauge. During sputtering, the Ar gas flow rate was adjusted using a 10 SCCM (SCCM denotes cubic centimeters per minute at STP) MKS flow controller, keep the Ar pressure constant with the main valve to the cryopump closed and the bypass valve open. In this configuration, the ion gauge reading of 4.5×10^{-5} mbar is approximately 100 times lower than the chamber pressure, which requires a few milliton to maintain a stable plasma discharge of the magnetron guns. The MgO(100) samples obtained from Princeton Scientific were mounted on a custom built sample platen made of pure titanium. The substrates were attached to the platen using thin Ta wires that were spot welded across the corners. Six filaments from 500 W halogen light bulbs were used to make the sample heater element. The samples could be routinely heated to temperatures of as high as 750 °C with this setup.

Two models of sputtering guns from AJA International, Inc., were used to deposit the films. The A300 series sputter gun uses a 1.5 in. target and requires a 4.5 in. CF flange to hold the assembly. The A310-XP gun utilizes a 1 in. target and can be attached to a 2.75 in. CF flange, making it more economical for sputtering precious metals. The ADAM system was equipped with four 1.5 in. sputter guns arranged in a square cluster, each directed at a 45° angle to the surface normal of the substrate at a working distance of 6 in.. A single 1 in. gun at the center of the four gun cluster is directed normal to the surface at a working distance of 5 in.. The sputter guns were powered using Advanced Energy MDX 500 supplies in constant power mode. The guns are arranged such that the substrate is at the focus of the cluster. The sample thickness variation was within 5% over a 1×1 in.^{2} area. The samples used in the experiments were either 1×1 or 2×2 cm^2.

The sputtering rates of pure elements were measured with a Leybold quartz crystal microbalance, which was translated to the sample position using a Huntington Mechanical Laboratories PMZ Manual Linear Z Motion Stage. The sputtering rates of alloy targets were measured using x-ray reflectivity. The composition of the alloy films was varied by adjusting the relative sputter rates of the magnetron guns containing an elemental target of Pt and an alloy target of $Fe_{50}Pt_{50}$. The magnetron guns were operated under conditions such that the sputter rate was directly proportional to the power supplied to the sputter gun. Table I defines various parameters used for flux calibration. As an example, $Fe_{50}Pt_{50}$ and Pt are considered with the respective parameters grouped in columns.

The mass ratio is given by

$$\frac{m_{FePt}}{m_{Pt}}=\frac{R_{FePt}D_{FePt}T}{R_{Pt}D_{Pt}T}, \tag{1}$$

where R_i is the sputtering rate for target i, D_i is the mass density of target i, and T is the deposition time. The mass

TABLE I. Definition of parameters in the sputter rate calibration of FePt and Pt.

Element	Sputter rate	Density	Atomic mass	Deposition time	Mass deposited per unit area	Mass in 1 mole of Fe_xPt_{100-x}
Fe	R_{Fe}	D_{Fe}	M_{Fe}	T	$m_{Fe}=R_{Fe}D_{Fe}$	xM_{Fe}
Pt	R_{Pt}	D_{Pt}	M_{Pt}		$m_{Pt}=R_{Pt}D_{Pt}$	$(100-x)M_{Pt}$

ratio in Eq. (1) is dictated by the required atomic composition for a particular alloy, Fe_xPt_{100-x}. The mass ratio is computed as

$$\frac{m_{FePt}}{m_{Pt}} = \frac{xM_{FePt}}{(100-2x)M_{Pt}}, \tag{2}$$

where M_i is the atomic mass of the target. Using Eq. (3), the rate ratio [Eq. (1)] can be written as

$$R_{FePt} = \frac{xM_{FePt}D_{Pt}}{(100-2x)M_{Pt}D_{FePt}}R_{Pt}. \tag{3}$$

Equation (3) defines the rate of $Fe_{50}Pt_{50}$ that must be used in conjunction with the rate of Pt (fixed) to achieve a particular atomic concentration of Fe in the alloy, x. A typical calibration curve for deposition rate of $Fe_{50}Pt_{50}$ measured by x-ray reflectivity as a function of applied power is shown in Fig. 2. For the samples produced in this study, a 1 in. $Fe_{50}Pt_{50}$ target was cosputtered with pure Pt to produce $Fe_{25}Pt_{75}$ using the above procedure. The sputtering rate of Pt is fixed to 0.32 A/s. According to Eq. (3), the sputtering rate of $Fe_{50}Pt_{50}$ should be 0.28 A/s to give the desired stoichiometry.

The growth temperature is controlled using a radiative heater powered by an ac power supply. A Philips X'Pert x-ray diffractometer with Cu $K\alpha$ radiation was used to perform structural characterization of the samples. For the modulated growth temperature sample, polarized neutron reflectivity measurements were performed at the Magnetism Reflectometer at the Spallation Neutron Source in Oak Ridge National Laboratory.

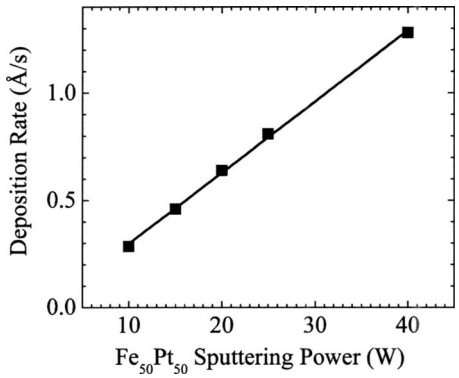

FIG. 2. Relationship between deposition rate and magnetron power for $Fe_{50}Pt_{50}$. The rate is determined by dividing the film thickness determined by x-ray reflectivity by the deposition time.

III. RESULTS

Figure 3 shows x-ray diffraction results for four films, with films (a)–(c) having a $Fe_{25}Pt_{75}$ thickness of 30 nm and film (d) with a $Fe_{25}Pt_{75}$ thickness of 150 nm. For the chemically disordered fcc structure, the (001) diffraction peak is forbidden since the diffraction peak indices *hkl* must be all even or all odd for the structure factor to be nonzero. The relative intensity of the (001) diffraction peak relative to the (002) diffraction peak is a direct measure of the amount of chemical order in the film. The intensity ratio for the (001) and (002) diffraction peaks corresponding to complete chemically ordered $FePt_3$ can be calculated by considering atomic fractions, atomic scattering factors, Debye–Waller corrections, Lorentz polarization factors, and structure factors and film thickness correction factor.[9,10]

The relative intensity of each peak can be expressed as

$$I = |F|^2 \times \Lambda \times G_t, \tag{4}$$

where F is the structure factor, Λ is the Lorenz polarization factor, and G_t is the film thickness correction factor.

The structure factor F's for (002) and (001) peaks are given by

$$F = \begin{cases} (f_{Fe}+i\delta_{Fe})e^{-W_{Fe}} + 3(f_{Pt}+i\delta_{Pt})e^{-W_{Pt}} & \text{for (002) peak} \\ (f_{Pt}+i\delta_{Pt})e^{-W_{Pt}} - (f_{Fe}+i\delta_{Fe})e^{-W_{Fe}} & \text{for (001) peak} \end{cases}, \tag{5}$$

where $f_{Fe(Pt)}$ and $\delta_{Fe(Pt)}$ represent the real and imaginary parts of the atomic scattering factors for Fe(Pt) and $e^{-W_{Fe(Pt)}}$ represents the Debye–Waller corrections for Fe(Pt).

For an epitaxial film, the Lorentz polarization Factor, Λ, is expressed as[11]

$$\Lambda = \frac{1+\cos^2(2\theta)}{\sin(2\theta)}, \tag{6}$$

where 2θ is the scattering angle.

The film thickness correction factor is given by[10]

$$G_t = 1 - \exp\left(-\frac{2\mu t}{\sin\theta}\right), \tag{7}$$

where μ is the linear absorption coefficient and t is the film thickness.

The parameters used to calculate ratio of (001) and (002) peak intensities for fully ordered $FePt_3$ are shown in Table II. For a 30 nm film, the calculated intensity ratio is $I_{001}:I_{002}=1:4.4$ and for a 150 nm film, this ratio is 1:3.9. A complete chemically ordered film has order parameter $S=1$ and a

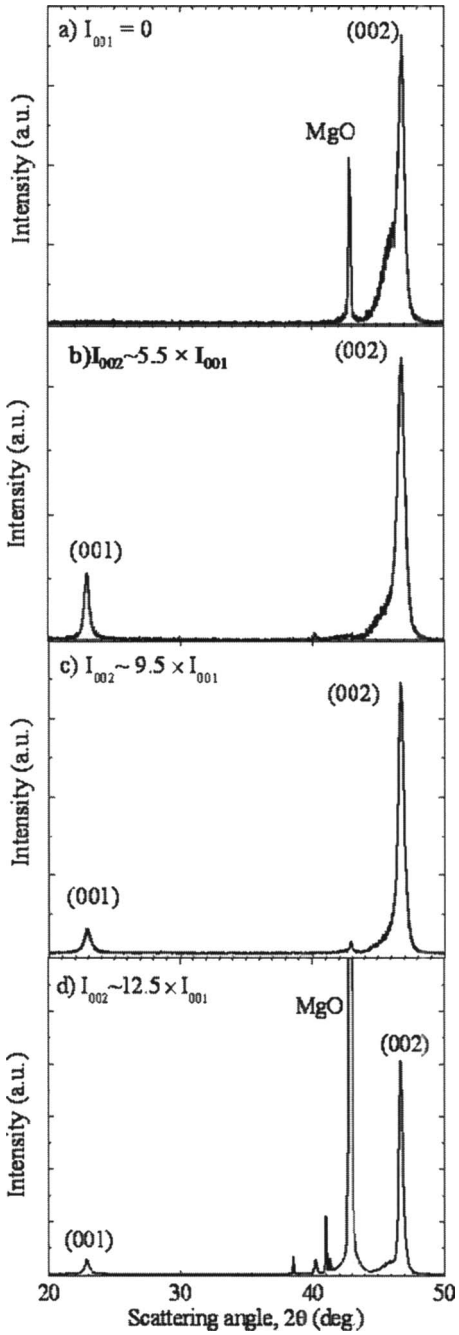

FIG. 3. X-ray diffraction data for (a) 30 nm deposited at 400 °C, (b) 30 nm deposited at 600 °C, (c) 20 nm deposited at 600 °C, followed by 10 nm deposited at 400 °C, and (d) a five-period superlattice of 20 nm deposited at 600 °C, followed by 10 nm deposited at 400 °C.

chemically disordered film an order parameter $S=0$. In between, the order parameter can be calculated from the intensity ratio by using

$$S^2 = \frac{(I_{001}/I_{002})_{\text{expt}}}{(I_{001}/I_{002})^{S=1}_{\text{calc.}}}. \tag{8}$$

Here, $(I_{001}/I_{002})_{\text{expt}}$ represents the intensity ratios from the measurement and $(I_{001}/I_{002})^{S=1}_{\text{calc.}}$ represents the calculated intensity ratio of peak intensity for a complete chemically ordered $FePt_3$.

For the film deposited at 400 °C, the intensity of the (001) peak is zero, so the film is completely disordered. So 400 °C is close to the highest growth temperature that does not produce significant chemical ordering. In Fig. 3(b), the film deposited at 600 °C has an intensity ratio of 1/5.5, which corresponds to an order parameter of 0.89. This temperature was selected as the high temperature of our modulated structure to minimize the time it takes to change the temperature between individual layers. Almost perfect order, $S=0.99$, is obtained for a film deposited at 700 °C, but it takes nearly twice as long to cool the sample to 400 °C from this temperature. Our prior results of neutron scattering measurements of the antiferromagnetic order in these materials have shown that the presence of chemical order is directly correlated to the existence of antiferromagnetic phases within the material.[12,13]

In Fig. 3(c), ideally, the film would be composed of 20 nm of $Fe_{25}Pt_{75}$ deposited at 600 °C and 10 nm deposited at 400 °C, with an order parameter of $S=0.89\times 2/3=0.60$. Using Eq. (5), the ratio of 1/9.5 from the measurement and the ratio of 1/4.4 from calculation for fully ordered $FePt_3$ with the same thickness, we obtain an order parameter of $S=0.68$, experimentally. This clearly shows that the bilayer film has a different order parameter as a result of a change in temperature during growth. The amount of order is higher than expected considering that only the portion of the film deposited at higher temperature exhibits order. The reason for the difference is that part of the 10 nm disordered $Fe_{25}Pt_{75}$ was deposited while the temperature was decreasing. It is necessary to continue the deposition while the temperature decreases to minimize interface contamination from residual gasses. If the transition region is assumed to have a linearly decreasing order parameter, then a transition thickness of about 5 nm is consistent with an order parameter of 0.68.

To perform neutron reflectivity measurements, it is desirable to have a periodic variation in the film structure with a few repeats. The repeat periodicity must correspond to the inverse of the momentum transfer range of the instrument to

TABLE II. Parameters used to calculate (001) and (002) peak intensities for fully ordered $FePt_3$.

Peak	θ	Λ	W_{Fe}	f_{Fe}	δ_{Fe}	W_{Pt}	f_{Pt}	δ_{Pt}	μ (cm^{-1})
(001)	11.45	4.75	0.0064	21.01	3.4	0.0064	64.43	8	3668
(002)	23.4	2.015	0.023	16.93	3.3	0.022	55.12	7	3668

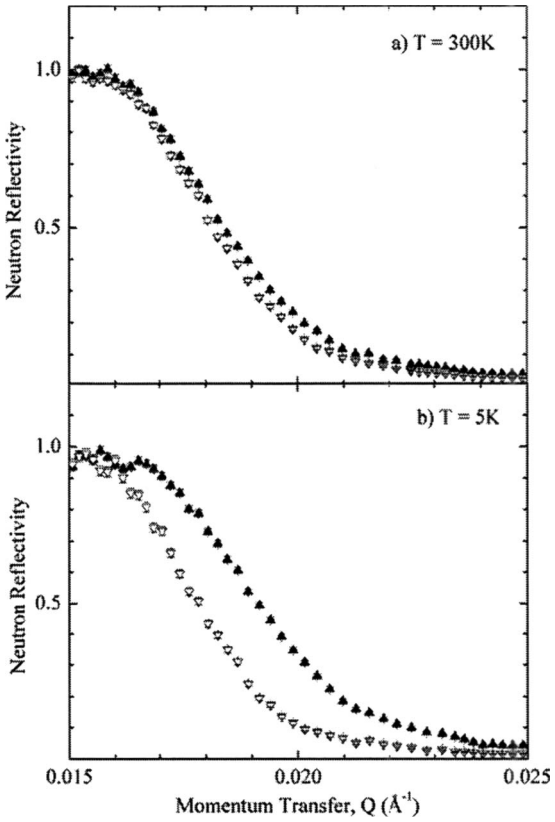

FIG. 4. Neutron reflectivity of the critical edge of a growth temperature-modulated superlattice showing the increase in magnetic splitting as the sample is cooled. The dark triangles are R^{++} and the open triangles are R^{--}.

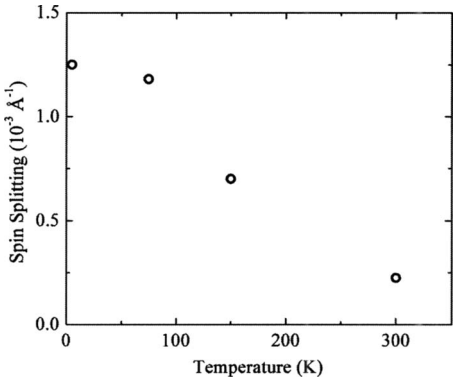

FIG. 5. Spin splitting of the polarized neutron reflectivity curves as a function of measurement temperature. The splitting at 300 K is 20% of the 5 K value, consistent with a ferromagnetic Curie temperature of approximately 350 K.

enable the observation of Bragg peaks in the reflectivity data. We chose to fabricate a five period superlattice for this purpose and the x-ray diffraction data for the superlattice film is shown in Fig. 3(d). From the data we calculate an order parameter of $S=0.56$ for this film. For this sample, the temperature change was programed such that the transition region extended into the high- and low-temperature deposited regions. In addition, it takes about twice as much time to cool down as it does to heat up the sample. The calculated order parameter is consistent with a film consisting of repeats of the following structure: 15 nm $FePt_3$ at 600 °C/5 nm $FePt_3$ while cooling from 600 to 400 °C/7 nm $FePt_3$ at 400 °C/3 nm $FePt_3$ while heating from 400 to 600 °C.

Figure 4 shows polarized neutron reflectivity measurements of sample (d) at low temperature and room temperature. The critical edge, defined as the momentum transfer at the point where the reflectivity drops to 0.5, is a direct measure of the neutron scattering density of the material.

Neutron scattering density has both a chemical and magnetic contribution, and the magnetic contribution can be positive or negative, depending on the relative orientations of neutron spin and sample magnetization. In the polarized neutron reflectivity measurement, the polarization of the neutrons is flipped relative to the magnetization of the sample and the observed difference in the critical edges is a direct measure of the magnetization of the sample. At 300 K, the splitting is nearly zero corresponding to a small residual magnetization of the sample near the Curie temperature. When the sample is cooled to $T=5$ K, the larger magnetic splitting indicates that the sample has a ferromagnetic component, which can be correlated with the ferromagnetism of the disordered component of the sample.[14]

Figure 5 shows the temperature dependence of the spin splitting for the superlattice. The splitting drops dramatically near room temperature, which is consistent with ferromagnetic Curie temperatures of 360–425 K for bulk alloys.[6] A reduced Curie temperature of 255 K has recently been observed in $Fe_{25}Pt_{75}$ nanocubes produced by chemical synthesis methods.[15] More detailed measurements to determine the magnetic parameters of the supperlattice structures are underway.

IV. CONCLUSIONS AND FUTURE WORK

We have shown that samples with a modulated order parameter, along the growth direction, can be produced by varying the substrate temperature during growth. X-ray diffraction measurements confirm that the amount of order is consistent with growth temperature changes for a bilayer film, and in the case of a superlattice, the measured value is about 20% lower than expected. Neutron reflectivity measurements confirm the ferromagnetism of the film at low temperature and a Curie temperature slightly above 300 K. We plan to examine a more complete set of polarized neutron reflectivity data to determine if Bragg peaks corresponding to the expected modulation period of the magnetic superlattice can be observed and correlated to the expected AF/FM structure.

ACKNOWLEDGMENTS

Part of this research was performed at the Spallation Neutron Source, supported by the Scientific User Facilities Division, Office of Basic Energy Sciences, Department of Energy. This research was funded by the NSF Materials Research Science and Engineering Center program through Grant No. NSF-DMR 0213985 and by the DOE/EPSCOR program under Grant No. DE-FG02-08ER46499.

[1]F. Radu and H. Zabel, in *Magnetic Heterostructures*, Springer Tracts in Modern Physics edited by H. Zabel, Samuel D. Bader (Springer, Berlin, 2008), Vol. 227, p. 97.
[2]R. Stamps, J. Phys. D **33**, R247 (2000).
[3]J. Nogués and I. K. Schuller, J. Magn. Magn. Mater. **192**, 203 (1999).
[4]C. Chappert, A. Fert, and F. N. Van Dau, Nature Mater. **6**, 813 (2007).
[5]S. Parkin, Xin Jiang, C. Kaiser, A. Panchula, K. Roche, and M. Samant, Proc. IEEE **91**, 661 (2003).
[6]G. E. Bacon and J. Crangle, Proc. R. Soc. London, Ser. A **272**, 387 (1963).
[7]D. Palaith, C. W. Kimball, R. S. Preston, and J. Crangle, Phys. Rev. **178**, 795 (1969).
[8]S. Maat, O. Hellwig, G. Zeltzer, Eric E. Fullerton, G. J. Mankey, M. L. Crow, and J. L. Robertson, Phys. Rev. B **63**, 134426 (2001).
[9]A. Cebollada, D. Weller, J. Sticht, G. R. Harp, R. F. C. Farrow, R. F. Marks, R. Savoy, and J. C. Scott, Phys. Rev. B **50**, 3419 (1994).
[10]S. Okamoto, O. Kitakami, and Y. Shinada, J. Magn. Magn. Mater. **208**, 102 (2000).
[11]B. E. Warren, *X-Ray Diffraction* (Dover, New York, 1990), p. 208.
[12]P. Mani, V. V. Krishnamurthy, S. Maat, A. J. Kellock, J. L. Robertson, and G. J. Mankey, J. Vac. Sci. Technol. A **23**, 785 (2005).
[13]P. Mani, V. V. Krishnamurthy, J. L. Robertson, F. Klose, and G. J. Mankey, J. Appl. Phys. **99**, 08C109 (2006).
[14]D. Lott, F. Klose, H. Ambaye, G. J. Mankey, P. Mani, M. Wolff, A. Schreyer, H. M. Christen, and B. C. Sales, Phys. Rev. B **77**, 132404 (2008).
[15]O. Margeat, M. Tran, M. Spasova, and M. Farle, Phys. Rev. B **75**, 134410 (2007).